Molecular Pharmacology Fast Forward. Published on February 25, 2015 as DOI: 10.1124/mol.115.098202
This article has not been copyedited and formatted. The final version may differ from this version.

EP2 receptor signaling regulates microglia death

Yujiao Fu, Myung-Soon Yang, Jianxiong Jiang, Thota Ganesh, Eunhye Joe, Raymond Dingledine

Department of Pharmacology, Emory University School of Medicine, Atlanta, Georgia, US (Y.F., M.-S.Y., J.J., T.G., R.D.); Neurology Department, Xiangya Hospital, Hunan, China (Y.F.); and Department of Pharmacology, Ajou University School of Medicine, Suwon, Korea (M.-S.Y., E.J.); Present address: Division of Pharmaceutical Sciences, James L. Winkle College of Pharmacy, University of Cincinnati, Cincinnati, OH, USA (J.J)

Molecular Pharmacology Fast Forward. Published on February 25, 2015 as DOI: 10.1124/mol.115.098202
This article has not been copyedited and formatted. The final version may differ from this version.

Running title: EP2 promotes microglia death

Correspondence should be addressed to:

Yujiao Fu

Department of Pharmacology

Emory University School of Medicine

Atlanta, GA 30322

Phone: 404-376-8697

E-mail: yujiao.fu@gmail.com

Number of text pages: 33

Number of tables: 0

Number of figures: 8

Number of references: 49

Number of words: Abstract 244

Introduction 715

Discussion 1228

ABBREVIATIONS:

AH6809, 6-isopropoxy-9-oxoxanthene-2-carboxylic acid; BHA, butylated hydroxyanisole; Calcein-AM, calcein-acetoxymethyl ester; CO, carbon monoxide; CoPP, cobalt protoporphyrin; CORM, carbon monoxide releasing molecule; CT, cycle threshold; FBS, fetal bovine serum; FRET, fluorescence resonance energy transfer; IL, interleukin; LPS, lipopolysaccharide; MEM, minimum Eagle's medium; NAC, N-acetyl cysteine; ONO-8711, 6-[(2R, 3S)-3-[[[(4-chloro-2-methylphenyl)sulfonyl]amino]methyl]bicyclo[2.2.2]oct-2-yl]-5Z-hexenoic acid; PBS, phosphate-buffered saline; qRT-PCR, quantitative real-time polymerase chain reaction; ROS, reactive oxygen species; SC-51089, 8-chloro-2-[1-oxo-3-(4-pyridinyl)propyl]hydrazide-dibenz[b,f][1,4]oxazepine-10(11H)-carboxylic acid, monohydrochloride; SE, status epilepticus; TG4-155, (E)-N-(2-(2-methyl-1H-indol-1-yl)ethyl)-3-(3,4,5-trimethoxyphenyl)acrylamide; TG7-170, N-(2-(2-methyl-1H-indol-1-yl)ethyl)-4-morpholinobenzamide; TG6-10-1, (E)-N-(2-(2-(trifluoromethyl)-1H-indol-1-yl)ethyl)-3-(3,4,5-trimethoxyphenyl)acrylamide.

Molecular Pharmacology Fast Forward. Published on February 25, 2015 as DOI: 10.1124/mol.115.098202
This article has not been copyedited and formatted. The final version may differ from this version.

ABSTRACT

The timely resolution of inflammation prevents continued tissue damage after an initial insult. In the brain the death of activated microglia by apoptosis has been proposed as one mechanism to resolve brain inflammation. How microglia death is regulated after activation is still unclear. We reported that exposure to lipopolysaccharide (LPS) and interleukin-13 (IL-13) together initially activates and then kills rat microglia in culture by a mechanism dependent on cyclooxygenase-2 (COX-2). We show here that activation of the prostaglandin E receptor 2 (EP2, or *PTGER2*) for prostaglandin E2 mediates microglia death induced by LPS/IL-13, and that EP2 activation by agonist alone kills microglia. Both EP2 antagonists and reactive oxygen scavengers block microglial death induced by either LPS/IL-13 or EP2 activation. By contrast the homeostatic induction of heme oxygenase 1 (Hmox1) by LPS/IL-13 or EP2 activation protects microglia. Both the Hmox1 inducer cobalt protoporphyrin (CoPP) and a compound that releases the Hmox1 product carbon monoxide (CO) attenuated microglial death produced by LPS/IL-13. Whereas CO reduced COX-2 protein expression, EP2 activation increased Hmox1 and COX-2 expression at both mRNA and protein level. Interestingly, caspase-1 inhibition prevented microglia death induced either by LPS/IL-13 or low (but not high) concentrations of butaprost, suggestive of a predominantly pyroptotic mode of death. Butaprost also caused the expression of activated caspase-3 in microglia pointing to apoptosis. These results indicate that EP2 activation, which initially promotes microglia activation, later causes delayed death of activated microglia, potentially contributing to the resolution phase of neuroinflammation.

Molecular Pharmacology Fast Forward. Published on February 25, 2015 as DOI: 10.1124/mol.115.098202
This article has not been copyedited and formatted. The final version may differ from this version.

Introduction

Microglia, the major innate immune cell type in the brain, respond to neuronal injury or prolonged seizures by transitioning from a resting to a classically activated state characterized by increased phagocytotic activity and release of numerous inflammatory molecules (Ransohoff and Cardona, 2010). Prompt resolution of inflammation once the original stimulus has been quenched is important to prevent a state of chronic inflammation that can lead to additional tissue injury and dysfunction. The processes by which inflammation is resolved in peripheral tissues such as lung are known to include apoptotic death of activated macrophages (Marriott et al., 2006). Like macrophages, activated microglia can be driven into apoptosis, which has been proposed to contribute to a return to the resting state (Yang et al., 2002). Mechanisms controlling microglial apoptosis are incompletely characterized but important to protect the brain from entering a state of chronic inflammation.

A number of pathways appear to control the entry of activated microglia into cell death programs. One microglial apoptotic pathway involves toll-like receptor 4 (TLR4) – mediated formation of interferon–β and subsequent engagement of caspases 11 and 3 (Jung et al., 2005). Another is triggered by formation of IL-13 by activated microglia (Shin et al., 2004), followed by induction of Jun kinase (JNK, or MAPK8) and consequent induction of COX-2. The resulting synthesis of PGE2 causes microglial death (Yang et al., 2006). IL-13 is a canonical type 2 cytokine produced by many cell types that induces a state of alternative activation in macrophages and microglia (Van Dyken and Locksley, 2013). In classically activated microglia IL-13 also opposes the induction of a major anti-oxidant protein, heme oxygenase-1 (Hmox1), and the resulting oxidative stress might contribute to development of the apoptotic state of microglia (Liu et al., 2010).

We were intrigued by results supporting the notion that enhanced death of activated microglia caused by IL-13 potentially involves activation of EP2 receptors (Yang et al., 2006). Endogenously activated by PGE2, EP2 is a Gαs-coupled receptor that signals by cyclic AMP

Molecular Pharmacology Fast Forward. Published on February 25, 2015 as DOI: 10.1124/mol.115.098202
This article has not been copyedited and formatted. The final version may differ from this version.

formation, and in some cases via β-arrestin (Chu et al., 2014). The activation of Epac by cAMP underlies much of the immunomodulatory role of EP2 in classically-activated microglia (Quan et al., 2013). Here we ask i) whether a selective EP2 antagonist prevents microglial cell death triggered by IL-13 and LPS, ii) whether EP2 influences the production of Hmox1 protein in activated microglia, iii) whether apoptosis and/or pyroptosis contributes to microglial death caused by EP2 activation, and iv) whether generation of reactive oxygen species contributes to microglial death caused by IL-13 and LPS, or EP2 activation. The results indicate a powerful role for EP2 activation in autoregulatory death of microglia.

Materials and methods

Reagents and Solutions

Lipopolysaccharide (LPS), Carbon monoxide releasing molecule (CORM) tricarbonyldichlororuthenium (II) dimer, bilirubin (BR), FeSO4, Ac-YVAD-cmk, N-acetyl cysteine (NAC) and butylated hydroxyanisole (BHA) were purchased from Sigma. Recombinant rat GM-CSF, and Z-WEHD-FMK were from R&D Systems. Recombinant rat IL-13 was from Peprotech. Cobalt protoporphyrin (CoPP) was from Porphyrin Products. Butaprost, 17-phenyl trinor Prostaglandin E2 ethyl amide, and ONO-8711 (6-[(2R,3S)-3-[[[(4-chloro-2-methylphenyl)sulfonyl]amino]methyl]bicyclo[2.2.2]oct-2-yl]-5Z-hexenoic acid) were from Cayman Chemicals. SC-51089 (8-chloro-2-[1-oxo-3-(4-pyridinyl)propyl]hydrazide-dibenz[b,f][1, 4]oxazepine-10(11H)-carboxylic acid, monohydrochloride) was from ENZO Life Sciences. MEM, Fetal Bovine Serum, and Penicillin-Streptomycin were from Gibco. HEPES was from GE Healthcare Hyclone (Logan, UT). Calcein-acetoxymethyl ester (calcein-AM) and ethidium homodimer-1 (Etd-1) for measurement of cell death were from Molecular Probes. The novel EP2 antagonists TG4-155 ((E)-N-(2-(2-methyl-1H-indol-1-yl)ethyl)-3-(3,4,5-trimethoxyphenyl)acrylamide), TG7-170 (N-(2-(2-methyl-1H-indol-1-yl)ethyl)-4-

Molecular Pharmacology Fast Forward. Published on February 25, 2015 as DOI: 10.1124/mol.115.098202
This article has not been copyedited and formatted. The final version may differ from this version.

morpholinobenzamide) and TG6-10-1 ((E)-N-(2-(2-(trifluoromethyl)-1H-indol-1-yl)ethyl)-3-(3,4,5-trimethoxyphenyl)acrylamide) were synthesized in our laboratory.

Microglial Cell Culture

Pregnant Sprague-Dawley rats were from Charles River Laboratories. Primary microglia were prepared from the cortex of 1 to 3-day old Sprague-Dawley rats as described previously (Quan et al., 2013). In brief, cortical tissue was carefully freed from blood vessels and meninges, triturated, and washed. Cortical cells were cultured in MEM, 10% FBS with penicillin/streptomycin plus 2 ng/ml GM-CSF for 10–14 days, during which medium was changed every 2–3 days. Microglia were then separated from the underlying astrocytic monolayer by gentle agitation. The cell pellet was resuspended in MEM, 5% FBS with penicillin/streptomycin but lacking GM-CSF and plated on cell culture plates (Corning). Non-adherent cells were removed after 30–60 min by changing the medium, and then adherent microglia were incubated for 24 h in culture medium before being exposed to drugs. Such cultures consist of >95% Iba1-positive microglia.

Seizure model and drug administration

Male C57Bl/6 mice (8-12 weeks old) from Charles River were housed under a 12-h light/dark cycle with food and water *ad libitum*. To minimize peripheral side effects of pilocarpine, mice were injected with methylscopolamine and terbutaline (2 mg/kg each in saline, i.p.). After 15-30 min pilocarpine (280 mg/kg in saline, freshly prepared, i.p.) was injected to induce status epilepticus (SE). Control mice received methylscopolamine and terbutaline but no pilocarpine. Seizures were classified as previously described (Borges et al., 2003; Jiang et al., 2012; Jiang et al., 2013). 0: normal behavior - walking, exploring, sniffing, grooming; 1: immobile, staring, jumpy, curled-up posture; 2: automatisms - repetitive blinking, chewing, head bobbing, vibrissae twitching, scratching, face-washing, “star-gazing”; 3: partial body clonus, occasional myoclonic

Molecular Pharmacology Fast Forward. Published on February 25, 2015 as DOI: 10.1124/mol.115.098202
This article has not been copyedited and formatted. The final version may differ from this version.

jerks, shivering; 4: whole body clonus, “corkscrew” turning & flipping, loss of posture, rearing and falling; 5: (SE onset): non-intermittent seizure activity; 6: wild running, bouncing, tonic seizures; 7: death. Mice underwent SE for 1 h, and SE was then terminated by pentobarbital (30 mg/kg in saline, i.p.). After 3 h mice were randomized and received three doses of vehicle (10% DMSO, 50% PEG 400, 40% ddH_2O) or TG6-10-1 (5 mg/kg, i.p.) at 4, 21 and 30 h after SE onset. Mice were fed moistened rodent chow, monitored daily and injected with 5% dextrose in lactated Ringer's solution (Baxter) (0.5 ml, s.c.) when necessary. One day and four days after SE groups of mice were euthanized under deep isoflurane anesthesia and perfused with phosphate buffered saline (PBS) to wash blood out of the brain. Hippocampal tissues were then collected for measuring mRNA levels. All experiments were approved by the Institutional Animal Care and Use Committee (IACUC) of Emory University and conducted in accordance with its guidelines. Every effort was made to minimize animal suffering.

Live and Dead Cell Assay

Viability of microglia was assessed by double-labeling of cells with 2 μM Calcein-AM and 4 μM Ethidium homodimer (Etd-1). Cells were counted using a Zeiss Axio Observer A1 fluorescence microscope (Zeiss, Germany), and judged as being alive or dead from their color and shape by eye. Cells that were stained only red by Etd-1, or stained both green and red, or stained very bright green with a small round shape were counted as dead cells, whereas cells that were stained only green by Calcein-AM and were not small round and bright were counted as live cells. In each condition 600-900 cells were counted in eight fields from two different wells. Some of the data was analyzed in a blinded fashion (in Figs 2A and 6A), and an excellent correlation was found between the scores from two independent raters of 28 images (Pearson’s correlation = 0.97); one of the raters in this test was unaware of the treatment conditions.

Quantitative real-time PCR (qRT-PCR)

Molecular Pharmacology Fast Forward. Published on February 25, 2015 as DOI: 10.1124/mol.115.098202
This article has not been copyedited and formatted. The final version may differ from this version.

Total RNA from microglia culture or mouse hippocampus was isolated using TRIzol (Invitrogen) with the PureLink RNA Mini Kit (Invitrogen). RNA concentration and purity were measured by A260 value and A260/A280 ratio, respectively. First-strand complementary DNA (cDNA) synthesis was performed with 1 μg of total RNA, 200 units of SuperScript II Reverse Transcriptase (Invitrogen), and 0.25 μg random primers in a reaction volume of 20 μl at 42°C for 50 min. The reaction was terminated by heating at 70°C for 15 min. qRT-PCR was performed by using 8 μl of 50× diluted cDNA, 0.4 μM of primers, and 2× B-R SYBR® Green SuperMix (Quanta BioSciences) with a final volume of 20 μl in the iQ5 Multicolor Real-Time PCR Detection System (Bio-Rad Laboratories). Cycling conditions were as follows: 95 °C for 2 min followed by 40 cycles of 95 °C for 15 s and then 60 °C for 1 min. Melting curve analysis was used to verify single-species PCR products. Fluorescent data were acquired at the 60 °C step. The geometric mean of the cycle thresholds for β-actin, GAPDH and HPRT1 was subtracted from the cycle threshold measured for each gene of interest to yield ΔCT. Samples without cDNA template served as the negative controls. Primers used for qRT-PCR were as follows: β-actin, forward 5'-CCAACCGTGAAAAGATGACC-3' were and reverse 5'- ACCAGAGGCATACAGGGACA -3' ; GAPDH, forward 5'- GGTGAAGGTCGGTGTGAAC -3' and reverse 5'-CCTTGACTGTGCCGTTGAA -3'; HPRT1, forward 5'- GGTCCATTCCTATGACTGTAGATTTT -3' and reverse 5'- CAATCAAGACGTTCTTTCCAGTT-3'; rat Hmox1, forward 5'-ACGAGGTGGGAGGTACTCAT-3' and reverse 5'- GCAGCTCCTCAAACAGCTCAA-3'; mouse Hmox1, forward 5'- GGAAATCATCCCTTGCACGC-3' and reverse 5'-TGTTTGAACTTGGTGGGGCT-3'; rat caspase-1, forward 5'- GAGCTTCAGTCAGGTCCATCA-3' and reverse 5'- AGGTCAACATCAGCTCCGAC-3'.

Time-resolved FRET cAMP Assay

cAMP levels in microglia were measured with a homogeneous time-resolved FRET method (Cisbio Bioassays), as described by Quan et al. (2013). The assay is based on generation of a

Molecular Pharmacology Fast Forward. Published on February 25, 2015 as DOI: 10.1124/mol.115.098202
This article has not been copyedited and formatted. The final version may differ from this version.

strong FRET signal upon the interaction of two molecules: an anti-cAMP antibody coupled to a FRET donor (cryptate) and cAMP coupled to a FRET acceptor (d2). Endogenous cAMP produced by cells competes with labeled cAMP for binding to the cAMP antibody and thus reduces the FRET signal, so the decrease of FRET signal indicates the increase of endogenous cAMP production. Briefly, microglia were seeded into 384-well plates in 30 µl of complete medium (6,000 cells/well) and grown overnight. Then cells were incubated with vehicle or 100 ng/ml LPS for 24 h. The medium was thoroughly withdrawn, and 10 µl of Hanks' buffered salt solution (Hyclone) plus 20µM rolipram was added into the wells to block phosphodiesterase. The cells were incubated at room temperature for 30 min and then treated with different concentrations of butaprost for 40 min. The cells were lysed in 10 µl of lysis buffer containing the FRET acceptor cAMP-d2, and 1 min later another 10 µl of lysis buffer with anti-cAMP-cryptate was added. After a 60–90 min incubation at room temperature, the time-resolved FRET signal was detected by an Envision 2103 multilabel plate reader (PerkinElmer Life Sciences) with laser excitation at 337 nm and dual emissions at 665 and 590 nm for d2 and cryptate, respectively. The FRET signal in Fig 1 was scaled between its maximum and minimum levels.

Western Blot

After being seeded in 6-well plates (500,000 cells/well), rat microglia received various treatments for indicated times and the cells were lysed on ice in RIPA buffer (Thermo Scientific) containing a mixture of protease and phosphatase inhibitors (Roche Applied Science). The lysate was centrifuged (12,000× g, 15 min, 4°C) and protein concentration in the supernate was measured by Bradford assay (Thermo Fisher Scientific). The supernates (30 µg protein each) were resolved by 12.5% sodium dodecyl sulfate polyacrylamide gel electrophoresis (SDS-PAGE) and electroblotted onto PVDF membranes (Millipore). Membranes were blocked with 5% non-fat milk at room temperature for 2 h, then incubated overnight at 4°C with primary antibodies: rabbit anti-Hmox1 (1:1,000, Santa Cruz Biotechnology), rabbit anti-caspase-1 (1:200, Santa Cruz

Molecular Pharmacology Fast Forward. Published on February 25, 2015 as DOI: 10.1124/mol.115.098202
This article has not been copyedited and formatted. The final version may differ from this version.

Biotechnology), goat anti-IL1 β (1:2,000, R&D system), or mouse anti- β -actin (1:16,000, Abcam). This procedure was followed by incubation with horseradish peroxidase-conjugated secondary antibodies (1:3,000, Santa Cruz Biotechnology) at room temperature for 2 h. The blots were developed by enhanced chemiluminescence (ECL) (Thermo Fisher Scientific).

Immunocytochemistry

Primary rat microglia were seeded in 24-well plates (100,000 cells/well) with coverslips on the bottom of each well. The coverslips were pre-coated with Poly-L-lysine (0.01%, Sigma-Aldrich). After incubation with drugs, cells were rinsed with ice cold PBS, fixed with 4% paraformaldehyde for 20 min, washed three times with PBS, blocked for 2 h in PBS/10% goat serum/ 0.2% triton X-100, and incubated overnight with the primary antibody, rabbit anti-cleaved caspase-3 (1:300, Cell Signaling Technology). After washing three times with PBS/ 0.2% triton X-100, the cells were incubated with Alexa Fluor goat anti-rabbit (1:1000, Molecular Probes, Eugene, OR) for 1 h at room temperature. The cells were washed three times with PBS, and nuclei were counterstained with 4',6-diamidino-2-phenylindole (Vectashield Mounting Medium with DAPI; Vector Laboratories, Burlingame, CA) for 30 min. Fluorescence images were acquired using a Zeiss Axio Observer A1 fluorescence microscope. In control experiments, the cells were processed in a similar manner except the primary antibodies were omitted. All negative controls showed no staining (data not shown).

Hmox1 activity assay

Hmox1 enzyme activity was measured as previously described (Kutty and Maines, 1982). Cytosolic extracts were prepared as described by Deveraux et al. (Deveraux et al., 1997). Briefly, rat liver was homogenized with ice-cold buffer A (20 mM HEPES, pH7.5, 10 mM KCl, 1.5 mM $MgCl_2$, 1 mM EDTA, 1 mM DTT), washed twice, and pelleted by centrifugation. Cell pellets were resuspended in one volume of buffer A, incubated for 30 min on ice, and disrupted by 20

Molecular Pharmacology Fast Forward. Published on February 25, 2015 as DOI: 10.1124/mol.115.098202
This article has not been copyedited and formatted. The final version may differ from this version.

passages through a 26-gauge needle. Cell extract supernatant was recovered after centrifuging at 100,000 X g for 1h at 37 °C. Microsomes from harvested cells were added to a reaction mixture containing NADPH (0.8 mM), rat liver cytosol (2 mg) as a source of biliverdin reductase, the substrate hemin (10 μM), glucose-6-phosphate (2 mM), and glucose-6-phosphate dehydrogenase (0.2 U). The reaction was carried out in the dark for 1 h at 37 °C, and terminated by the addition of 500 μl chloroform. Hmox1 activity is showed as pmole of bilirubin/mg of protein/60 min.

Statistics

Data are shown as mean ± SEM; n = number of independent experiments with each condition typically run in duplicate or triplicate, except Fig. 1, where the means of n=3 or 4 technical replicates are shown in a single experiment. Comparisons are made by ANOVA with correction for multiple comparisons as noted in the figure legends, or by 1-sample t-test in Figs 1A and 7D.

Results

Activation of *EP2 receptors underlies microglial death induced by LPS/IL-13*

We have previously reported that COX-2 inhibitors prevent the death of rat microglia that occurs several days after exposure to a combination of IL-13 and the inflammatory trigger, LPS, and that a nonselective EP1/EP2 antagonist (AH6809, 6-isopropoxy-9-oxoxanthene-2-carboxylic acid) reduced cell death (Yang et al., 2006). COX-2 is dramatically up-regulated and leads to PGE2 synthesis during inflammation (Murakami et al., 2000; Quan et al., 2013). PGE2 activates four different G protein-coupled receptors designated EP1, EP2, EP3, EP4 (Narumiya et al., 1999). Cultured rat microglia were reported to express EP1, EP2 and EP4, but not the EP3 receptor subtype (Caggiano and Kraig, 1999; Shi et al., 2010). We confirmed the presence

Molecular Pharmacology Fast Forward. Published on February 25, 2015 as DOI: 10.1124/mol.115.098202
This article has not been copyedited and formatted. The final version may differ from this version.

of EP2 receptors by qRT-PCR, and interestingly, we found that incubation with LPS (10 or 100 ng/ml) for 24 h dose-dependently increased EP2 mRNA level in rat microglia (Fig. 1A). Further, to explore whether LPS alters the response of microglia to the EP2 agonist butaprost, we incubated rat primary microglia cultures with vehicle or 100 ng/ml LPS for 24 h followed by addition of different concentrations of butaprost for 2 h. Butaprost activates EP2 to increase intracellular cyclic adenosine monophosphate (cAMP) in rat microglia. Cellular cAMP levels were evaluated by a time-resolved FRET assay (Jiang et al., 2010) (Fig. 1B). LPS at 100 ng/ml produced an 8-fold shift to the left in the concentration-response curve of butaprost, reducing its EC_{50} from 644 nM in resting microglia to 84.4 nM in LPS-activated microglia.

To explore which prostaglandin receptor is involved in regulating microglia death, we examined the effects of selective EP1 and EP2 antagonists (Jiang et al., 2012) and agonists on microglia death. Butaprost selectively activates EP2, whereas 17-phenyl trinor-PGE_2 activates EP1 and EP3 and increases intracellular [Ca^{2+}] in rat astrocytes with an EC50 of 69 nM (Kiriyama et al., 1997). TG4-155 and TG7-170 are selective EP2 antagonists synthesized in our laboratory (Ganesh et al., 2014a; Ganesh et al., 2014b) (Fig. 2A), and Sc-51089 and ONO-8711 are selective EP1 antagonists (Hallinan et al., 1996; Watanabe et al., 1999). Both EP2 antagonists reduced LPS/IL-13 induced microglia death, whereas high concentrations of EP1 antagonists caused an insignificant reduction of cell death (Fig. 2B and C). The observed trend for reduction of microglia death caused by EP1 antagonists might be explained by weak inhibition of EP2 receptors or a small contribution of EP1 receptor signaling. Additionally, the EP2 agonist butaprost itself dose-dependently induced rat microglia death and this was reduced by both EP2 antagonists, but the EP1 agonist 17-phenyl trinor-PGE2 at 2 μM did not influence microglia cell viability (Fig. 2D-F). Those data together indicate that EP2 receptors are induced by microglial activation, and that EP2 activation contributes to microglia death that is produced by prolonged exposure to LPS and IL-13. Microglial death caused by butaprost occurred more

Molecular Pharmacology Fast Forward. Published on February 25, 2015 as DOI: 10.1124/mol.115.098202
This article has not been copyedited and formatted. The final version may differ from this version.

quickly than that caused by LPS/IL-13, hence we selected different exposure times to measure microglial death in Fig 2.

Reactive oxygen species (ROS) mediate death of microglia induced by LPS/IL-13 or EP2 activation

ROS have been reported to mediate cell death by apoptosis or programmed necrosis in different cell types (Bartlett et al., 2013; Fortes et al., 2012; Hollensworth et al., 2000; Hou et al., 2005; Noguchi et al., 2008; Won et al., 2013). Two ROS scavengers, N-acetyl-L-cysteine (NAC) and butylated hydroxyanisole (BHA), were chosen to determine whether ROS is involved in microglia death induced by exposure to LPS/IL-13 or butaprost. NAC is a thiol precursor of L-cysteine and reduced glutathione. It is a source of sulfhydryl groups in cells and a scavenger of free radicals, interacting with ROS such as OH• and H_2O_2 (Aruoma et al., 1989). BHA, another well-known ROS scavenger, can trap chain-carrying peroxy radicals ($ROO_•$) by donation of its phenolic hydrogen. Rat microglia were preincubated with NAC (1 or 10 mM) or BHA (1 or 10 μM) for 2 h followed by addition of LPS (10 ng/ml) plus IL-13 (20 ng/ml) for 6 days, or followed by EP2 agonist butaprost (200 nM) for 3 days. Microglia were stained with Calcein-AM and the DNA intercolator Etd-1, cells were imaged and counted as either live or dead (Fig. 3A). Following treatment, NAC and BHA dose-dependently reduced microglia death induced by either LPS/IL-13 or butaprost (Fig. 3). This result indicates that reactive oxygen species are involved in microglia death induced either by LPS/IL-13 or EP2 activation. Phase contrast images were taken with a Zeiss Axio Observer A1 fluorescence microscope after the different treatments (Fig. 3E). Microglia in both LPS and LPS/IL-13 group initially became swollen and round compared with the typically elongated cells in the control condition, however cell shrinkage was seen in LPS/IL-13 group from day 3 suggesting apoptosis. Likewise, exposure to butaprost (2, 20 and especially 200 nM for 2 days) also caused microglia to shrink.

Molecular Pharmacology Fast Forward. Published on February 25, 2015 as DOI: 10.1124/mol.115.098202
This article has not been copyedited and formatted. The final version may differ from this version.

With CO involved, the antioxidant Hmox1 opposes microglia death induced by LPS/IL-13

Heme-oxygenase 1 (Hmox1) is a metabolic enzyme that utilizes NADPH and oxygen to break apart the heme moiety liberating carbon monoxide (CO), iron and biliverdin, which is subsequently converted to bilirubin (Fig. 4A). CO has profound effects on mitochondria, cellular respiration and other hemoproteins to which it can bind; CO and bilirubin are both potent antioxidants. Sequestration of iron into ferritin and its recycling in the tissues is part of a homeodynamic process that controls oxidation-reduction in cellular metabolism. We confirmed (Liu et al., 2010) that LPS-induced Hmox1 expression is reduced by IL-13 (Supplemental Figure 1A), and we also found that LPS-increased Hmox1 activity was reduced by IL-13, determined by measuring bilirubin production (Supplemental Figure 1B). Live and dead cell assay was then performed to determine whether the replenishment of Hmox1 activity attenuated LPS/IL-13 induced microglial death. Microglia were incubated for 6 days with 10 ng/ml LPS, 20 ng/ml IL-13, and cobalt protoporphyrin (CoPP), a well-known Hmox1 inducer (Cai et al., 2012). CoPP reduced LPS/IL-13 induced microglia death (Fig. 4B), indicating that microglial death is exacerbated by down-regulation of Hmox1. Next, we examined which enzymatic product of Hmox1 was involved in protecting microglia from death. Microglia were exposed for 6 days to LPS, IL-13, and tricarbonyldichlororuthenium (II) dimer used as a source of CO (CO-releasing molecule, CORM) or bilirubin or Fe^{2+}, then mortality was assessed. CORM but neither bilirubin nor Fe^{2+} caused a reduction in LPS/IL-13 induced microglia death (Fig. 4C-E). These results indicate that antioxidant Hmox1, with CO involved, opposes LPS/IL-13 induced microglia death.

EP2 signaling increases Hmox1 expression

Based on results that LPS/IL-13-induced microglia death is mediated by EP2 activation but opposed by Hmox1, we explored the interaction between Hmox1 and EP2. First, microglia were exposed to LPS, IL-13, and either CORM, bilirubin or Fe^{2+} for 3 days, and western blot

Molecular Pharmacology Fast Forward. Published on February 25, 2015 as DOI: 10.1124/mol.115.098202
This article has not been copyedited and formatted. The final version may differ from this version.

was performed to examine whether Hmox1's products influence IL-13-enhanced COX-2 expression. Only CORM, which rescued microglia from LPS/IL-13-induced death (Fig 4C), but not bilirubin or Fe^{2+}, was found to reduce COX-2 expression dose-dependently (Supplemental Figure 2). This result suggests that the down-regulation of COX-2 by Hmox1's product CO might contribute to reduced microglial death.

To determine whether EP2 activation affects the expression of Hmox1, microglia were preincubated with EP2 agonist butaprost (2 μM) for 1 h followed by addition of LPS (1 or 10 ng/ml) for 12h and 24h, and then mRNA and protein were isolated to measure Hmox1 expression. Interestingly, we found that butaprost potentiated induction of Hmox1 mRNA and protein by LPS, but butaprost alone was without effect (Fig. 5A-B), indicating that EP2 activation increases Hmox1 expression in activated but not resting microglia. This result was further expanded in C57BL/6 mice that underwent pilocarpine-induced status epilepticus (SE) (Fig. 5C-D). SE was allowed to proceed for 1 h and then terminated by pentobarbital. Three hours later (i.e., 4 h after SE onset), vehicle or TG6-10-1, which is a brain permeant EP2 antagonist, was administered (5 mg/kg, i.p.). Two additional doses of TG6-10-1 were administered at 21h and 30h after SE onset to approximately match the temporal pattern of COX-2 induction after pilocarpine (Jiang et al., 2015). One and four days after SE groups of mice were sacrificed and hippocampal tissue was isolated to measure Hmox1 mRNA level. Hmox1 mRNA was increased both one and four days after SE, and TG6-10-1 treatment decreased Hmox1 mRNA expression at both time points (Fig 5C, D). These data indicate that EP2 activation increases Hmox1 expression both in vitro and in vivo, which could serve as a homeostatic mechanism in microglia activation.

Role of caspases 1 and 3 in microglia death induced by LPS/IL-13 or butaprost

Molecular Pharmacology Fast Forward. Published on February 25, 2015 as DOI: 10.1124/mol.115.098202
This article has not been copyedited and formatted. The final version may differ from this version.

LPS/IL-13 induced microglia death was reported to have apoptotic characteristics – chromatin condensation and fragmentation, and positive TUNEL staining (Yang et al., 2002). Interleukin-1 converting enzyme (ICE, or caspase-1), which is an enzyme that cleaves the precursor forms of the inflammatory cytokines interleukin 1β and interleukin 18 into active mature peptides, is one component of the inflammasome that triggers pyroptosis. Pyroptosis is a form of programmed cell death initially associated with antimicrobial responses during inflammation (Aachoui et al., 2013). During pyroptosis cells swell, eventually lyse and release proinflammatory mediators. Caspase-1 can also promote apoptosis (Exline et al., 2014; Sarkar et al., 2006; Sollberger et al., 2015). We examined whether caspase-1 is involved in LPS/IL-13-induced microglia death. Rat microglia were preincubated with caspase-1 inhibitors Z-WEHD-FMK (20 μM) or Ac-YVAD-cmk (50 μM) for 4 h followed by addition of LPS/IL-13 for 6 days. Microglia were stained with Calcein-AM and Etd-1, cells were imaged and counted. Both Z-WEHD-FMK and Ac-YVAD-cmk greatly reduced microglia death (Fig. 6A), suggesting that caspase-1 is largely responsible for LPS/IL-13 induced microglia death. Z-WEHD-FMK also nearly eliminated microglial death induced by a low concentration (2 nM) of butaprost, but had no effect on death caused by 200 or 2000 nM butaprost (Fig 6B). Butaprost (2-2000 nM) induced the formation of activated caspase 3 (Fig. 6C), which is one of the key caspases responsible for cleavage of numerous cellular proteins, leading to the biochemical and morphological hallmarks of apoptosis (Brancolini et al., 1997). These results taken together suggest two modes of microglial death, pyroptosis at low levels of EP2 activation and predominantly apoptosis as EP2 activation increases.

EP2 activation reduces levels of both pro-capase-1 and pro-IL1β proteins

Since inhibitors of both EP2 and caspase-1 can nearly fully prevent LPS/IL-13 induced microglia death, we explored whether the EP2 agonist leads to caspase-1 activation, which cleaves pro-IL1β into mature IL1β. Primary rat microglia were preincubated with 2 μM butaprost

Molecular Pharmacology Fast Forward. Published on February 25, 2015 as DOI: 10.1124/mol.115.098202
This article has not been copyedited and formatted. The final version may differ from this version.

for 1 h followed by addition of LPS (10 ng/ml) for 12 and 24h, and then protein was isolated to analyze caspase-1 and IL-1β expression. Both pro-caspase-1 and pro-IL-1β were increased by LPS, and interestingly, both were decreased by the addition of butaprost (Fig. 7A,C). However, neither mature caspase-1 nor mature IL1β protein was detected (not shown). When microglia were preincubated with LPS (10 ng/ml) for 6 h followed by addition of 2 μM butaprost for indicated times, western blot showed that butaprost time-dependently reduced LPS-enhanced pro-IL1β expression (Fig. 7B), although again no mature IL-1β was detected. By contrast, butaprost increased the mRNA levels of both IL-1β (Quan et al., 2013) and caspase 1 in activated microglia (Fig. 7D).

Discussion

The major findings of this study are that i) EP2 signaling regulates the death of activated microglia, ii) cell death mediated by EP2 involves the activation of caspases 1 and 3 as well as the generation of reactive oxygen species, and iii) both activated microglia and EP2 activation engage an antioxidant Hmox1 pathway that opposes cell death. Microglial death induced by LPS+IL-13 was potentiated by butaprost and fully prevented by EP2 antagonists. Inhibition of caspase-1 could also fully prevent the death of activated microglia produced by IL-13 or weak EP2 activation by 2 nM butaprost, but interestingly caspase-1 inhibitors were ineffective against microglial death induced by strong EP2 activation. By contrast, EP2 activation by butaprost also caused a slowly developing apoptosis in resting microglia characterized by cell shrinkage and increased caspase-3 cleavage. Butaprost reduced the expression of pro-caspase-1 and pro-IL1β proteins in activated microglia while increasing their mRNA levels, which is consistent with the possibility that EP2 activation induces the formation of mature caspase-1 and IL-1β. A schematic diagram (Fig 8) shows a pro-death pathway initiated by TLR4 activation involving

Molecular Pharmacology Fast Forward. Published on February 25, 2015 as DOI: 10.1124/mol.115.098202
This article has not been copyedited and formatted. The final version may differ from this version.

COX-2 and EP2, which is opposed by a feedback / feedforward antioxidant pathway mediated by Hmox1 and its enzymatic product, CO. We propose that low levels of EP2 activation triggered by LPS + IL-13 engage mainly a caspase-1 death pathway, whereas this pyroptotic pathway is overridden by apoptosis potentially mediated by caspase-3 during strong EP2 activation (Fig 8). This situation is similar to the differential effect of low vs high NMDA receptor activation on two modes of neuronal death (Bonfoco et al., 1995).

EP2 receptors play an essential role in the regulation of inflammatory cytokine and chemokine expression in many different cell types including macrophages, microglia, and tumor cells (Jiang and Dingledine, 2013; Johansson et al., 2013). Examining both resting and LPS-activated microglia, we found that rat primary microglia up-regulate their EP2 receptors with a 4-fold increase in mRNA level and an 8-fold increase in agonist potency (Fig. 1). This result is different from our previous finding that the potency of EP2 receptors in rat microglia was similar between resting and activated state (Quan et al., 2013). These two findings can potentially be reconciled by different culture conditions – here we included 10% fetal bovine serum (FBS) but no GM-CSF in the media after cell plating. By enhancing the expression and potency of EP2 receptors upon insults, microglia can actively engage themselves in regulating critical inflammatory pathways with amplified signaling downstream of EP2 receptors. EP2 levels in vivo can also be dynamically regulated. The EP2 mRNA level in mouse hippocampus was increased 3-4 fold within 16 hr of status epilepticus and was associated with a strong inflammatory response although bulk EP2 protein levels were unchanged (Jiang et al., 2015). EP2 mediates pro-inflammatory effects in models of innate immunity (Ganesh et al., 2013), Alzheimer's Disease (Johansson et al., 2014), amyotrophic lateral sclerosis (Liang et al., 2008), and status epilepticus (Jiang et al., 2012; Jiang et al., 2013; Varvel et al., 2015). EP2 receptor antagonists quench neuroinflammation after status epilepticus (Jiang et al., 2012; Jiang et al.,

Molecular Pharmacology Fast Forward. Published on February 25, 2015 as DOI: 10.1124/mol.115.098202
This article has not been copyedited and formatted. The final version may differ from this version.

2013). Whether EP2 agonist potency itself is increased in these disease models and thus contributes to disease progression is an interesting question.

Death of activated microglia is one potential mechanism for resolution of inflammation. IL-13 promotes the death of LPS-activated microglia characterized by positive TUNEL staining and DNA fragmentation (Yang et al., 2002), together with caspase-12 mediated ER stress (Liu et al., 2010; Szegezdi et al., 2003), suggesting an apoptotic mode of microglia death. We found that microglia death induced by LPS/IL-13 was blocked by two caspase-1 inhibitors (Fig. 6A and B). The activation of caspase-1 is a key feature of inflammasome formation, which results in subsequent processing of IL-1β and IL-18 and can induce an inflammatory, lytic type of cell death known as pyroptosis. However, recent studies show that caspase-1 can also be involved in apoptosis. After intraperitoneal challenge of mice with live Escherichia coli, splenic B lymphocyte apoptosis was found in wild-type mice and both IL-1β knockout and IL-1β/IL-18 double knockout mice but not in caspase-1 knockout mice. Importantly, IL-1β/IL-18 double knockout mice were protected from splenic cell apoptosis by the pan-caspase inhibitor z-VAD-fmk (Sarkar et al., 2006). Caspase-1 inhibitor YVAD-cmk reduced human lymphocyte apoptosis in sepsis (Exline et al., 2014). The induction of caspase-1 precedes that of caspase-3 in UVB stimulated human keratinocytes, and cells with reduced caspase-1 expression show much less caspase-3 associated apoptosis (Sollberger et al., 2015). All these findings indicate that under certain conditions caspase-1 can induce caspase-3 activation, which can trigger subsequent apoptosis.

EP2 activation caused a mixed immune state in classically-activated microglia, exacerbating the rapid induction of some proinflammatory mediators (COX-2, IL-6, IL-1β) while blunting others (TNF-α, CCL3, CCL4), and thus EP2 regulates microglia activation (Quan et al., 2013). We confirmed the finding of Yang et al. (2006) that EP2 activation also dose-dependently

Molecular Pharmacology Fast Forward. Published on February 25, 2015 as DOI: 10.1124/mol.115.098202
This article has not been copyedited and formatted. The final version may differ from this version.

induces the death of resting microglia, and we show here that activation of both EP2 receptors and caspase 1 underlie the death of microglia caused by IL-13 (Fig. 2B, 6A,B). In addition butaprost can induce an apoptotic morphology of resting microglia, accompanied by increased caspase-3 cleavage (Fig. 6D) as well as DNA fragmentation and PARP cleavage (Nagano et al., 2014). The death of microglia caused by high concentrations of butaprost is dependent upon reactive oxygen species (Fig. 3D) and is completely blocked by an EP2 antagonist (Fig. 2F). In LPS-activated microglia, butaprost increases caspase-1 and IL-1β mRNA expression while reducing the protein levels of both pro-caspase-1 and pro-IL1β, consistent with the possibility that EP2 activation induces the formation of mature caspase-1 and IL1β from their precursor. However we were not able to detect mature caspase-1 or IL-1β by western blot and suspect that the mature forms were quickly degraded in our culture conditions. We propose that strong EP2 activation in resting microglia activates caspase-3 directly and produces apoptosis. By contrast in LPS-activated microglia with up-regulated EP2 receptors, weaker EP2 activation induces caspase-1 signaling, which then promotes pyroptosis or caspase-3 cleavage leading to apoptosis (Fig 8). At the same time, EP2 activation by butaprost exerts a negative feedback role by enhancing Hmox1 expression both in vitro and in vivo (Fig. 5A-D), which opposes activated microglia death (Fig 4B,C). Taken together, our results indicate that EP2 activation initially promotes microglia activation and then induces slow death either by pyroptosis or apoptosis. These conclusions are drawn from the effects of selective EP2 agonists and antagonists, and it would be worthwhile to confirm with microglia deficient in EP2 receptors (Johansson et al., 2013).

Considering the crucial role of EP2 signaling in regulating classical activation of microglia (Quan et al., 2013), we conclude that COX-2 dependent EP2 activation promotes microglia activation in early stages of inflammation and then causes a delayed death of activated microglia. Thus, as suggested by Yang et al. (2002), microglial death could be one event

Molecular Pharmacology Fast Forward. Published on February 25, 2015 as DOI: 10.1124/mol.115.098202
This article has not been copyedited and formatted. The final version may differ from this version.

underlying the resolution of neuroinflammation. Targeting EP2 signaling pathways may be an efficient approach to control the degree of microglia activation, thus reducing chronic inflammation and brain damage in neurological diseases. The therapeutic window for EP2 antagonists opens after seizures with the neuronal induction of COX-2 and consequent production of PGE2 (Jiang et al., 2015; Rojas et al., 2015). Our data suggest that the therapeutic window might close towards the end of active inflammation, when microglial death is needed to resolve inflammation.

Acknowledgements

We thank Asheebo Rojas, Nicholas Varvel, and Nadia Lelutiu for help and advice.

Authorship contributions

Participated in research design: Fu, Yang, Joe, and Dingledine

Conducted experiments: Fu, Yang, and Jiang

Performed data analysis: Fu, Yang, and Dingledine

Wrote or contributed to the writing of the manuscript: Fu, Yang, Jiang, Ganesh, and Dingledine.

Molecular Pharmacology Fast Forward. Published on February 25, 2015 as DOI: 10.1124/mol.115.098202
This article has not been copyedited and formatted. The final version may differ from this version.

References

Aachoui Y, Sagulenko V, Miao EA and Stacey KJ (2013) Inflammasome-mediated pyroptotic and apoptotic cell death, and defense against infection. *Current opinion in microbiology* **16**(3):319-326.

Aruoma OI, Halliwell B, Hoey BM and Butler J (1989) The antioxidant action of N-acetylcysteine: its reaction with hydrogen peroxide, hydroxyl radical, superoxide, and hypochlorous acid. *Free radical biology & medicine* **6**(6):593-597.

Bartlett R, Yerbury JJ and Sluyter R (2013) P2X7 receptor activation induces reactive oxygen species formation and cell death in murine EOC13 microglia. *Mediators of inflammation* **2013**:271813.

Bonfoco E, Krainc D, Ankarcrona M, Nicotera P and Lipton SA (1995) Apoptosis and necrosis: two distinct events induced, respectively, by mild and intense insults with N-methyl-D-aspartate or nitric oxide/superoxide in cortical cell cultures. *Proceedings of the National Academy of Sciences of the United States of America* **92**(16):7162-7166.

Borges K, Gearing M, McDermott DL, Smith AB, Almonte AG, Wainer BH and Dingledine R (2003) Neuronal and glial pathological changes during epileptogenesis in the mouse pilocarpine model. *Exp Neurol* **182**(1):21-34.

Brancolini C, Lazarevic D, Rodriguez J and Schneider C (1997) Dismantling cell-cell contacts during apoptosis is coupled to a caspase-dependent proteolytic cleavage of beta-catenin. *The Journal of cell biology* **139**(3):759-771.

Caggiano AO and Kraig RP (1999) Prostaglandin E receptor subtypes in cultured rat microglia and their role in reducing lipopolysaccharide-induced interleukin-1beta production. *Journal of neurochemistry* **72**(2):565-575.

Cai C, Teng L, Vu D, He JQ, Guo Y, Li Q, Tang XL, Rokosh G, Bhatnagar A and Bolli R (2012) The heme oxygenase 1 inducer (CoPP) protects human cardiac stem cells against apoptosis through

activation of the extracellular signal-regulated kinase (ERK)/NRF2 signaling pathway and cytokine release. *The Journal of biological chemistry* **287**(40):33720-33732.

Chu CH, Chen SH, Wang Q, Langenbach R, Li H, Zeldin D, Chen SL, Wang S, Gao H, Lu RB and Hong JS (2014) PGE2 Inhibits IL-10 Production via EP2-Mediated beta-Arrestin Signaling in Neuroinflammatory Condition. *Molecular neurobiology* **In press**.

Deveraux QL, Takahashi R, Salvesen GS and Reed JC (1997) X-linked IAP is a direct inhibitor of cell-death proteases. *Nature* **388**(6639):300-304.

Exline MC, Justiniano S, Hollyfield JL, Berhe F, Besecker BY, Das S, Wewers MD and Sarkar A (2014) Microvesicular caspase-1 mediates lymphocyte apoptosis in sepsis. *PloS one* **9**(3):e90968.

Fortes GB, Alves LS, de Oliveira R, Dutra FF, Rodrigues D, Fernandez PL, Souto-Padron T, De Rosa MJ, Kelliher M, Golenbock D, Chan FK and Bozza MT (2012) Heme induces programmed necrosis on macrophages through autocrine TNF and ROS production. *Blood* **119**(10):2368-2375.

Ganesh T, Jiang J, Shashidharamurthy R and Dingledine R (2013) Discovery and characterization of carbamothioylacrylamides as EP selective antagonists. *ACS medicinal chemistry letters* **4**(7):616-621.

Ganesh T, Jiang J, Yang MS and Dingledine R (2014a) Lead optimization studies of cinnamic amide EP2 antagonists. *Journal of medicinal chemistry* **57**(10):4173-4184.

Ganesh T, Jianxiong J and Dingledine R (2014b) Development of second generation EP2 antagonists with high selectivity. *Eur J Med Chem* **82**(521-535).

Hallinan EA, Hagen TJ, Tsymbalov S, Husa RK, Lee AC, Stapelfeld A and Savage MA (1996) Aminoacetyl moiety as a potential surrogate for diacylhydrazine group of SC-51089, a potent PGE2 antagonist, and its analogs. *Journal of medicinal chemistry* **39**(2):609-613.

Hollensworth SB, Shen C, Sim JE, Spitz DR, Wilson GL and LeDoux SP (2000) Glial cell type-specific responses to menadione-induced oxidative stress. *Free radical biology & medicine* **28**(8):1161-1174.

Hou RC, Wu CC, Huang JR, Chen YS and Jeng KC (2005) Oxidative toxicity in BV-2 microglia cells: sesamolin neuroprotection of H2O2 injury involving activation of p38 mitogen-activated protein kinase. *Annals of the New York Academy of Sciences* **1042**:279-285.

Jiang J and Dingledine R (2013) Role of prostaglandin receptor EP2 in the regulations of cancer cell proliferation, invasion, and inflammation. *The Journal of pharmacology and experimental therapeutics* **344**(2):360-367.

Jiang J, Ganesh T, Du Y, Quan Y, Serrano G, Qui M, Speigel I, Rojas A, Lelutiu N and Dingledine R (2012) Small molecule antagonist reveals seizure-induced mediation of neuronal injury by prostaglandin E2 receptor subtype EP2. *Proceedings of the National Academy of Sciences of the United States of America* **109**(8):3149-3154.

Jiang J, Ganesh T, Du Y, Thepchatri P, Rojas A, Lewis I, Kurtkaya S, Li L, Qui M, Serrano G, Shaw R, Sun A and Dingledine R (2010) Neuroprotection by selective allosteric potentiators of the EP2 prostaglandin receptor. *Proc Natl Acad Sci U S A* **107**(5):2307-2312.

Jiang J, Quan Y, Ganesh T, Pouliot WA, Dudek FE and Dingledine R (2013) Inhibition of the prostaglandin receptor EP2 following status epilepticus reduces delayed mortality and brain inflammation. *Proceedings of the National Academy of Sciences of the United States of America* **110**(9):3591-3596.

Jiang J, Quan Y, Yang MS, Gueorguieva P, Ganesh T, Rojas A, Lelutiu N and Dingledine R (2015) Therapeutic window for cyclooxygenase-2 related anti-inflammatory therapy after status epilepticus. *Neurobiol of Disease* **In press**.

Johansson JU, Pradhan S, Lokteva LA, Woodling NS, Ko N, Brown HD, Wang Q, Loh C, Cekanaviciute E, Buckwalter M, Manning-Bog AB and Andreasson KI (2013) Suppression of inflammation with conditional deletion of the prostaglandin E2 EP2 receptor in macrophages and brain microglia. *The Journal of neuroscience : the official journal of the Society for Neuroscience* **33**(40):16016-16032.

Johansson JU, Woodling NS, Wang Q, Panchal M, Liang X, Trueba-Saiz A, Brown HD, Mhatre SD, Loui T and Andreasson KI (2014) Prostaglandin signaling suppresses beneficial microglial function in Alzheimer's disease models. *The Journal of clinical investigation*.

Jung DY, Lee H, Jung BY, Ock J, Lee MS, Lee WH and Suk K (2005) TLR4, but not TLR2, signals autoregulatory apoptosis of cultured microglia: a critical role of IFN-beta as a decision maker. *Journal of immunology* **174**(10):6467-6476.

Kiriyama M, Ushikubi F, Kobayashi T, Hirata M, Sugimoto Y and Narumiya S (1997) Ligand binding specificities of the eight types and subtypes of the mouse prostanoid receptors expressed in Chinese hamster ovary cells. *British journal of pharmacology* **122**(2):217-224.

Kutty RK and Maines MD (1982) Oxidation of heme c derivatives by purified heme oxygenase. Evidence for the presence of one molecular species of heme oxygenase in the rat liver. *The Journal of biological chemistry* **257**(17):9944-9952.

Liang X, Wang Q, Shi J, Lokteva L, Breyer RM, Montine TJ and Andreasson K (2008) The prostaglandin E2 EP2 receptor accelerates disease progression and inflammation in a model of amyotrophic lateral sclerosis. *Annals of neurology* **64**(3):304-314.

Liu SH, Yang CN, Pan HC, Sung YJ, Liao KK, Chen WB, Lin WZ and Sheu ML (2010) IL-13 downregulates PPAR-gamma/heme oxygenase-1 via ER stress-stimulated calpain activation: aggravation of activated microglia death. *Cellular and molecular life sciences : CMLS* **67**(9):1465-1476.

Marriott HM, Hellewell PG, Cross SS, Ince PG, Whyte MK and Dockrell DH (2006) Decreased alveolar macrophage apoptosis is associated with increased pulmonary inflammation in a murine model of pneumococcal pneumonia. *Journal of immunology* **177**(9):6480-6488.

Murakami M, Naraba H, Tanioka T, Semmyo N, Nakatani Y, Kojima F, Ikeda T, Fueki M, Ueno A, Oh S and Kudo I (2000) Regulation of prostaglandin E2 biosynthesis by inducible membrane-associated prostaglandin E2 synthase that acts in concert with cyclooxygenase-2. *The Journal of biological chemistry* **275**(42):32783-32792.

Nagano T, Kimura SH and Takemura M (2014) Prostaglandin E2 induces apoptosis in cultured rat microglia. *Brain research* **1568**:1-9.

Narumiya S, Sugimoto Y and Ushikubi F (1999) Prostanoid receptors: structures, properties, and functions. *Physiological reviews* **79**(4):1193-1226.

Noguchi T, Ishii K, Fukutomi H, Naguro I, Matsuzawa A, Takeda K and Ichijo H (2008) Requirement of reactive oxygen species-dependent activation of ASK1-p38 MAPK pathway for extracellular ATP-induced apoptosis in macrophage. *The Journal of biological chemistry* **283**(12):7657-7665.

Quan Y, Jiang J and Dingledine R (2013) EP2 receptor signaling pathways regulate classical activation of microglia. *The Journal of biological chemistry* **288**(13):9293-9302.

Ransohoff RM and Cardona AE (2010) The myeloid cells of the central nervous system parenchyma. *Nature* **468**(7321):253-262.

Rojas A, Ganesh T, Lelutiu N, Gueorguieva P and Dingledine R (2015) Inhibition of prostaglandin EP2 receptor is neuroprotective and accelerates functional recovery in a rat model of organophosphate induced status epilepticus. *Neuropharmacology* **In press**.

Sarkar A, Hall MW, Exline M, Hart J, Knatz N, Gatson NT and Wewers MD (2006) Caspase-1 regulates Escherichia coli sepsis and splenic B cell apoptosis independently of interleukin-1beta and interleukin-18. *American journal of respiratory and critical care medicine* **174**(9):1003-1010.

Shi J, Johansson J, Woodling NS, Wang Q, Montine TJ and Andreasson K (2010) The prostaglandin E2 E-prostanoid 4 receptor exerts anti-inflammatory effects in brain innate immunity. *Journal of immunology* **184**(12):7207-7218.

Shin WH, Lee DY, Park KW, Kim SU, Yang MS, Joe EH and Jin BK (2004) Microglia expressing interleukin-13 undergo cell death and contribute to neuronal survival in vivo. *Glia* **46**(2):142-152.

Sollberger G, Strittmatter GE, Grossi S, Garstkiewicz M, dem Keller UA, French LE and Beer HD (2015) Caspase-1 Activity is Required for UVB-Induced Apoptosis of Human Keratinocytes. *The Journal of investigative dermatology* **In press**.

Szegezdi E, Fitzgerald U and Samali A (2003) Caspase-12 and ER-stress-mediated apoptosis: the story so far. *Annals of the New York Academy of Sciences* **1010**:186-194.

Van Dyken SJ and Locksley RM (2013) Interleukin-4- and interleukin-13-mediated alternatively activated macrophages: roles in homeostasis and disease. *Annual review of immunology* **31**:317-343.

Varvel NH, Jiang J and Dingledine R (2015) Candidate drug targets for prevention or modification of epilepsy. *Annual review of pharmacology and toxicology* **55**:229-247.

Watanabe K, Kawamori T, Nakatsugi S, Ohta T, Ohuchida S, Yamamoto H, Maruyama T, Kondo K, Ushikubi F, Narumiya S, Sugimura T and Wakabayashi K (1999) Role of the prostaglandin E receptor subtype EP1 in colon carcinogenesis. *Cancer research* **59**(20):5093-5096.

Won SY, Kim SR, Maeng S and Jin BK (2013) Interleukin-13/Interleukin-4-induced oxidative stress contributes to death of prothrombinkringle-2 (pKr-2)-activated microglia. *Journal of neuroimmunology* **265**(1-2):36-42.

Yang MS, Ji KA, Jeon SB, Jin BK, Kim SU, Jou I and Joe E (2006) Interleukin-13 enhances cyclooxygenase-2 expression in activated rat brain microglia: implications for death of activated microglia. *Journal of immunology* **177**(2):1323-1329.

Molecular Pharmacology Fast Forward. Published on February 25, 2015 as DOI: 10.1124/mol.115.098202
This article has not been copyedited and formatted. The final version may differ from this version.

Yang MS, Park EJ, Sohn S, Kwon HJ, Shin WH, Pyo HK, Jin B, Choi KS, Jou I and Joe EH (2002) Interleukin-13 and -4 induce death of activated microglia. *Glia* **38**(4):273-280.

Molecular Pharmacology Fast Forward. Published on February 25, 2015 as DOI: 10.1124/mol.115.098202
This article has not been copyedited and formatted. The final version may differ from this version.

Footnotes

This work was supported by the National Institutes of Health (NIH) [Grants R21NS074169, U01NS058158, P20NS080185], NARSAD Young Investigator Grant, and National Institute of Neurological Disorders and Stroke (NINDS) [Grants K99/R00NS082379].

Send reprint requests to:

Yujiao Fu

Department of Pharmacology

Emory University School of Medicine

Atlanta, GA 30322

Email: yujiao.fu@gmail.com

Molecular Pharmacology Fast Forward. Published on February 25, 2015 as DOI: 10.1124/mol.115.098202
This article has not been copyedited and formatted. The final version may differ from this version.

Figure Legends

FIGURE 1. **Expression and activity of EP2 receptors in primary rat microglia. A**, rat microglia were incubated with vehicle, 10 or 100 ng/ml LPS for 24h, and mRNA levels were measured by quantitative real-time PCR (qRT-PCR). The mRNA changes were normalized to the mean of the control group. Data were analyzed by one-sample t test with Bonferroni correction. Data are expressed as mean + S.E. (error bars), n=5. **, $p< 0.01$ versus control. **B**, Rat microglia were incubated with vehicle or 100ng/ml LPS for 24h followed by addition of different concentrations of butaprost for 2h. Cellular cAMP levels were evaluated by a TR-FRET assay. LPS caused a shift to the left in the butaprost concentration-response curve. Data points represent mean ± S.E. (error bars) from a single experiment run in triplicate. This experiment was repeated with essentially the same results.

FIGURE 2. **EP2 activation produced cell death in both resting and activated microglia. A**, the structure of EP2 antagonists TG4-155 and TG7-170. **B** and **C**, rat microglia were pretreated with antagonists for EP1 (Sc-51089 or ONO-8711) or EP2 (TG4-155, or TG7-170) receptors for 4h followed by addition of 10ng/ml LPS and 20ng/ml IL-13 for 6 days. Cell death was determined by staining with Calcein-AM and Etd-1. n=4-6. **D**, microglia were incubated with vehicle or agonists of EP1 (17-phenyl-trinor) or EP2 (butaprost) receptors for 3 days. Cell death was determined by staining. n=3-6. **E** and **F**, microglia were pretreated with vehicle or indicated concentrations of EP2 antagonist TG4-155 for 2h followed by 200nM butaprost for 3 days. Cell death was determined by staining. Representative images are shown, Scale bar = 100μm, n = 3-6. Data were analyzed by one-way ANOVA with Dunnett's test. Data are shown as mean + S.E. (error bars). *, $p< 0.05$; **, $p< 0.01$.

FIGURE 3. **Reactive oxygen species mediate microglia death induced by LPS/IL-13 or**

Molecular Pharmacology Fast Forward. Published on February 25, 2015 as DOI: 10.1124/mol.115.098202
This article has not been copyedited and formatted. The final version may differ from this version.

butaprost. Rat microglia were pretreated with vehicle or reactive oxygen species (ROS) scavengers BHA or NAC for 2h followed by addition of 10ng/ml LPS and 20ng/ml IL-13 for 6 days (**B** and **C**), or 200nM butaprost for 3 days (**D**). Cell death was measured by staining with Calcein-AM and Etd-1. Representative images are shown, Scale bar = 100μm (**A**). Data were analyzed by one-way ANOVA with post-hoc Bonferroni. Data are shown as mean + S.E. (error bars), n=3-6. **, $p< 0.01$ versus LPS/IL-13 or butaprost group. **E**, microglia were incubated with vehicle, 10 ng/ml LPS, or 10 ng/ml LPS plus 20 ng/ml IL-13 for 4 days, or 200nM butaprost for 3 days, and phase contrast images were taken with a Zeiss Axio Observer A1 fluorescence microscope; representative images are shown, n=6.

FIGURE 4. **Effects of Hmox1 inducer and its products on IL-13 induced death in activated rat microglia. A**, Hmox1 degrades heme into Fe^{2+}, CO and bilirudin, which is then converted to bilirubin. **B**-**E** Microglia were incubated with Hmox1 inducer CoPP or tricarbonyldichlororuthenium (II) dimer used as a source of CO (CO-releasing molecule, CORM) or bilirubin or Fe^{2+} , together with 10ng/ml LPS and 20ng/ml IL-13 for 6 days. Cell death was evaluated by staining with Calcein-AM and Etd-1. Data were analyzed by one-way ANOVA with post-hoc Bonferroni. Data are shown as mean + S.E. (error bars), n=6-8. *, $p< 0.05$; **, $p< 0.01$ versus LPS/IL-13 group.

FIGURE 5. **EP2 activation increases Homx-1 expression.** Rat microglia were pretreated with EP2 agonist butaprost for 1h followed by addition of 1ng/ml or 10ng/ml LPS for 12h and 24h. Cells were lysed to obtain total protein samples for Western Blot and mRNA samples for qRT-PCR. **A**, the changes in Hmox1 protein induced 12h and 24h after addition of 10ng/ml LPS. The data shown are representative of three independent experiments. **B**, the changes in Hmox1 mRNA 12h after addition of 1ng/ml LPS (n=5). **C** and **D**, the changes in Hmox1 mRNA in mouse hippocampi 1 and 4 days after status epilepticus measured by qRT-PCR (n=6-8). Data were

Molecular Pharmacology Fast Forward. Published on February 25, 2015 as DOI: 10.1124/mol.115.098202
This article has not been copyedited and formatted. The final version may differ from this version.

analyzed by one-way ANOVA with post-hoc Bonferroni test. Data are shown as mean + S.E. (error bars). **, p< 0.01; ***, p< 0.001.

FIGURE 6. **Involvement of caspases 1 and 3 in microglial death caused by LPS/IL-13 or butaprost. A**, rat microglia were pretreated with vehicle or caspase-1 inhibitors Ac-YVAD-cmk or Z-WEHD-FMK for 4h followed by addition of 10 ng/ml LPS and 20 ng/ml IL-13 for 6 days. Cell death was determined by staining with Calcein-AM and Etd-1. Representative images are shown, Scale bar = 100μm. Data were analyzed by one-way ANOVA with Dunnett's test. Data are expressed as mean + S.E. (error bars), n=4-6. **, p< 0.01. **B**, Microglia were incubated with the indicated concentrations of butaprost and the caspase 1 inhibitor for 3 days and microglial death assessed by the live/dead assay. Data are shown as mean + S.E, n=3; **, p<.01 by one-way ANOVA with post-hoc Bonferroni. **C**, rat microglia were incubated with vehicle or 2μM butaprost for indicated times. Microglia were fixed and stained for cleaved caspase-3 and nucleic acid (DAPI); representative images are shown, n=3. NS, not significant.

FIGURE 7. **Effect of EP2 activation on inflammasome signaling.** Rat microglia were pretreated with 2μM butaprost for 1h followed by 10ng/ml LPS for 12h and 24h, or microglia were incubated with 10ng/ml LPS for 6h followed by 2μM butaprost for 0.5-3h. Cells were lysed to obtain protein samples for Western Blot. **A** and **B**, the changes in pro-IL-1β protein induced 12h after LPS; no mature IL-1β was detected under any condition (not shown). **C**, changes in pro-caspase-1 protein induced 12h and 24h after LPS and butaprost; no mature caspase-1 was detected. These data are representative of three independent experiments. Fig. 7C and Fig. 5A were from the same blot that was stripped and reblotted so the β-actin loading controls are reproduced. **D**, microglia were pretreated with 2μM butaprost followed by addition of 1ng/ml LPS for 12h, and caspase-1 mRNA level was measured by qRT-PCR. The mRNA changes were normalized to the mean of the control group. Data were analyzed by one-sample t test with

Molecular Pharmacology Fast Forward. Published on February 25, 2015 as DOI: 10.1124/mol.115.098202
This article has not been copyedited and formatted. The final version may differ from this version.

Bonferroni correction. Data are expressed as mean + S.E. (error bars), n=5. *, p< 0.05 versus LPS group.

FIGURE 8. **Proposed role of EP2 and Hmox1 in death of activated microglia**. The proposed pathways are deduced from the current results as well as results presented in Yang et al. (2002).

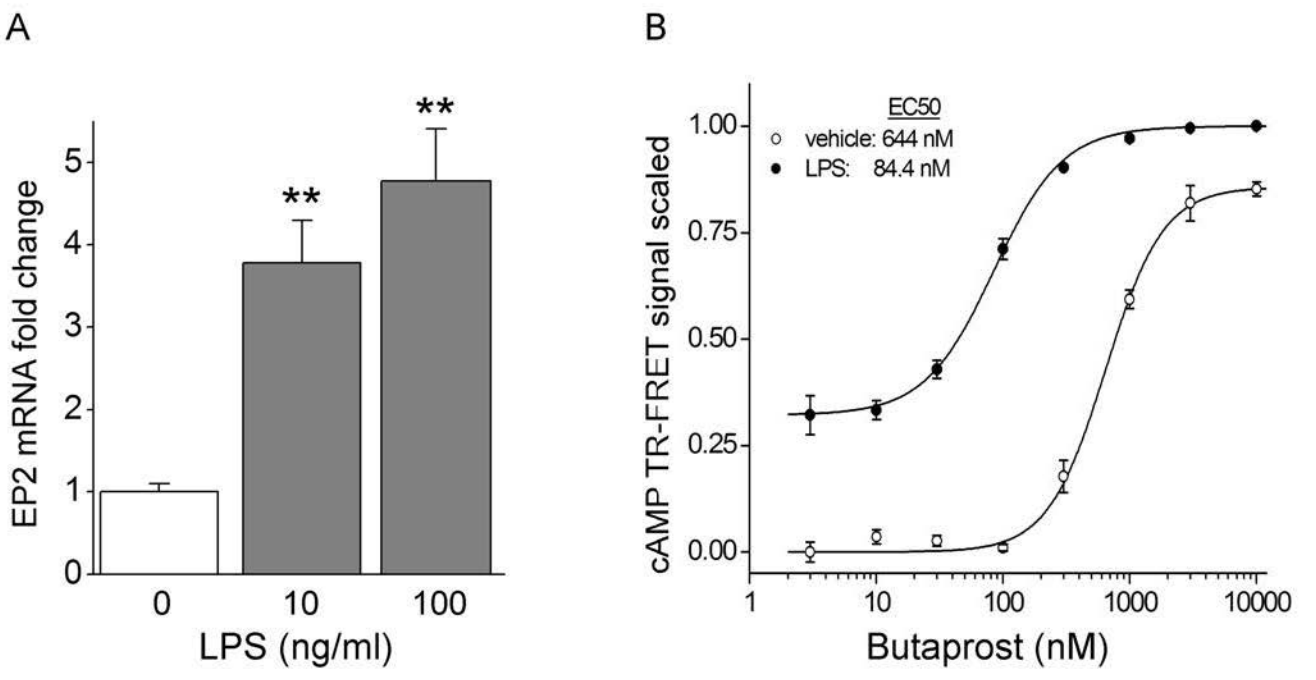
A
EP2 mRNA fold change
0
1
2
3
4
5
**
**
0
10
100
LPS (ng/ml)
B
cAMP TR-FRET signal scaled
0.00
0.25
0.50
0.75
1.00
EC50
vehicle: 644 nM
LPS: 84.4 nM
1
10
100
1000
10000
Butaprost (nM)

Figure 1

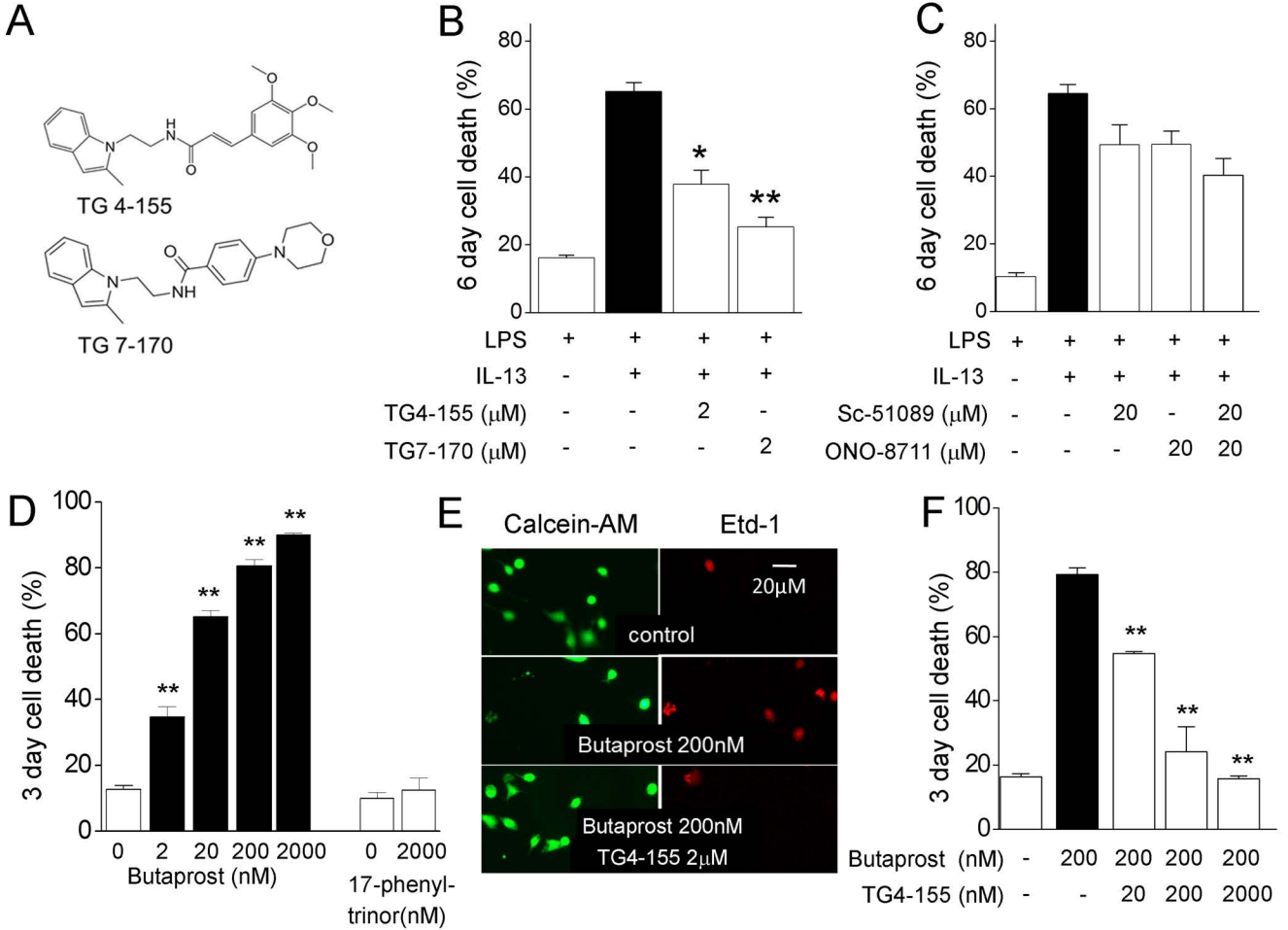
A
TG 4-155
TG 7-170
B
6 day cell death (%)
LPS
IL-13
TG4-155 (μM)
TG7-170 (μM)
C
6 day cell death (%)
LPS
IL-13
Sc-51089 (μM)
ONO-8711 (μM)
D
3 day cell death (%)
Butaprost (nM)
17-phenyl-trinor(nM)
E
Calcein-AM
Etd-1
20μM
control
Butaprost 200nM
Butaprost 200nM
TG4-155 2μM
F
3 day cell death (%)
Butaprost (nM)
TG4-155 (nM)

Figure 2

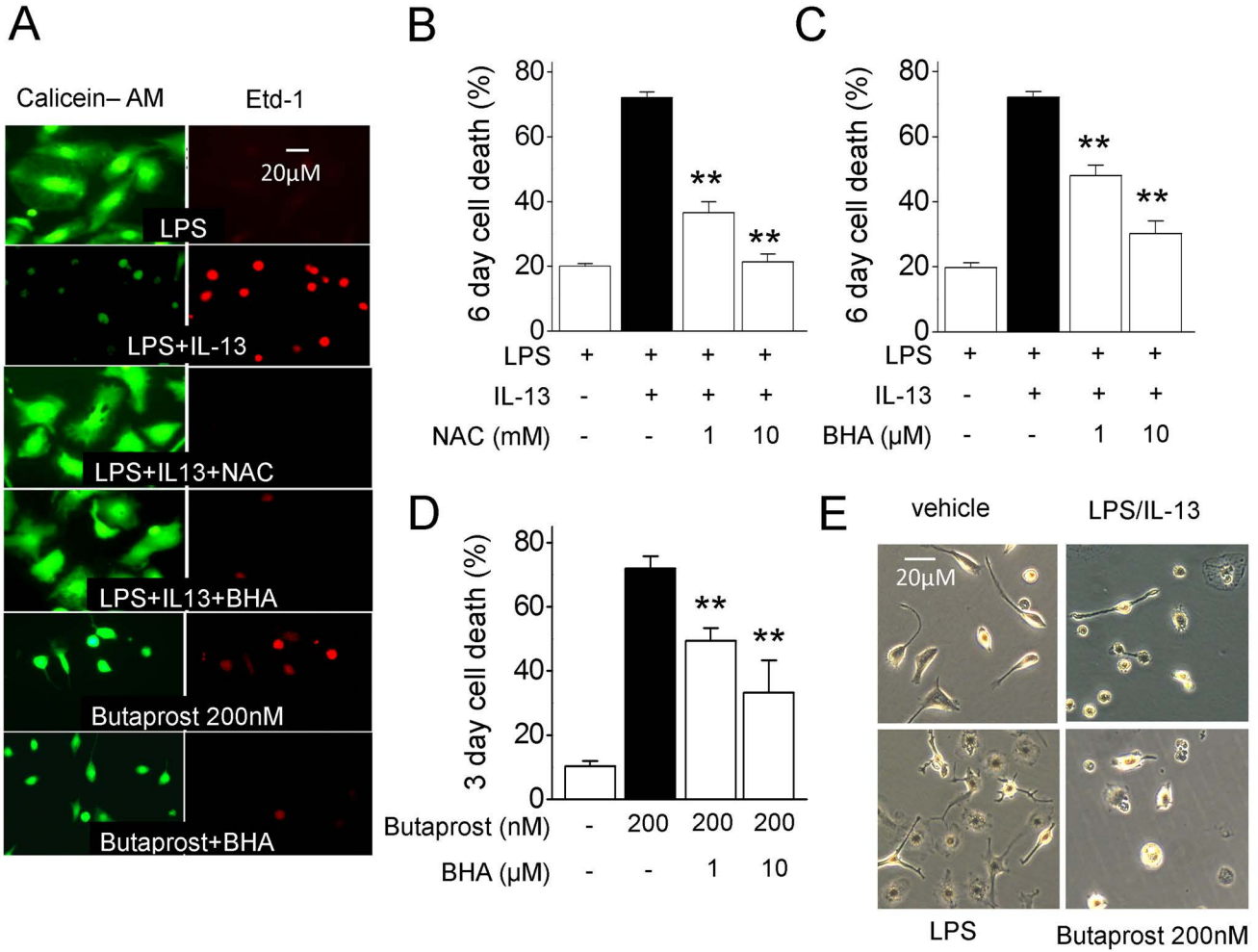
A
Calicein– AM
Etd-1
20μM
LPS
LPS+IL-13
LPS+IL13+NAC
LPS+IL13+BHA
Butaprost 200nM
Butaprost+BHA
B
6 day cell death (%)
80
60
40
20
0
**
**
LPS + + + +
IL-13 - + + +
NAC (mM) - - 1 10
C
6 day cell death (%)
80
60
40
20
0
**
**
LPS + + + +
IL-13 - + + +
BHA (μM) - - 1 10
D
3 day cell death (%)
80
60
40
20
0
**
**
Butaprost (nM) - 200 200 200
BHA (μM) - - 1 10
E
vehicle
LPS/IL-13
20μM
LPS
Butaprost 200nM

Figure 3

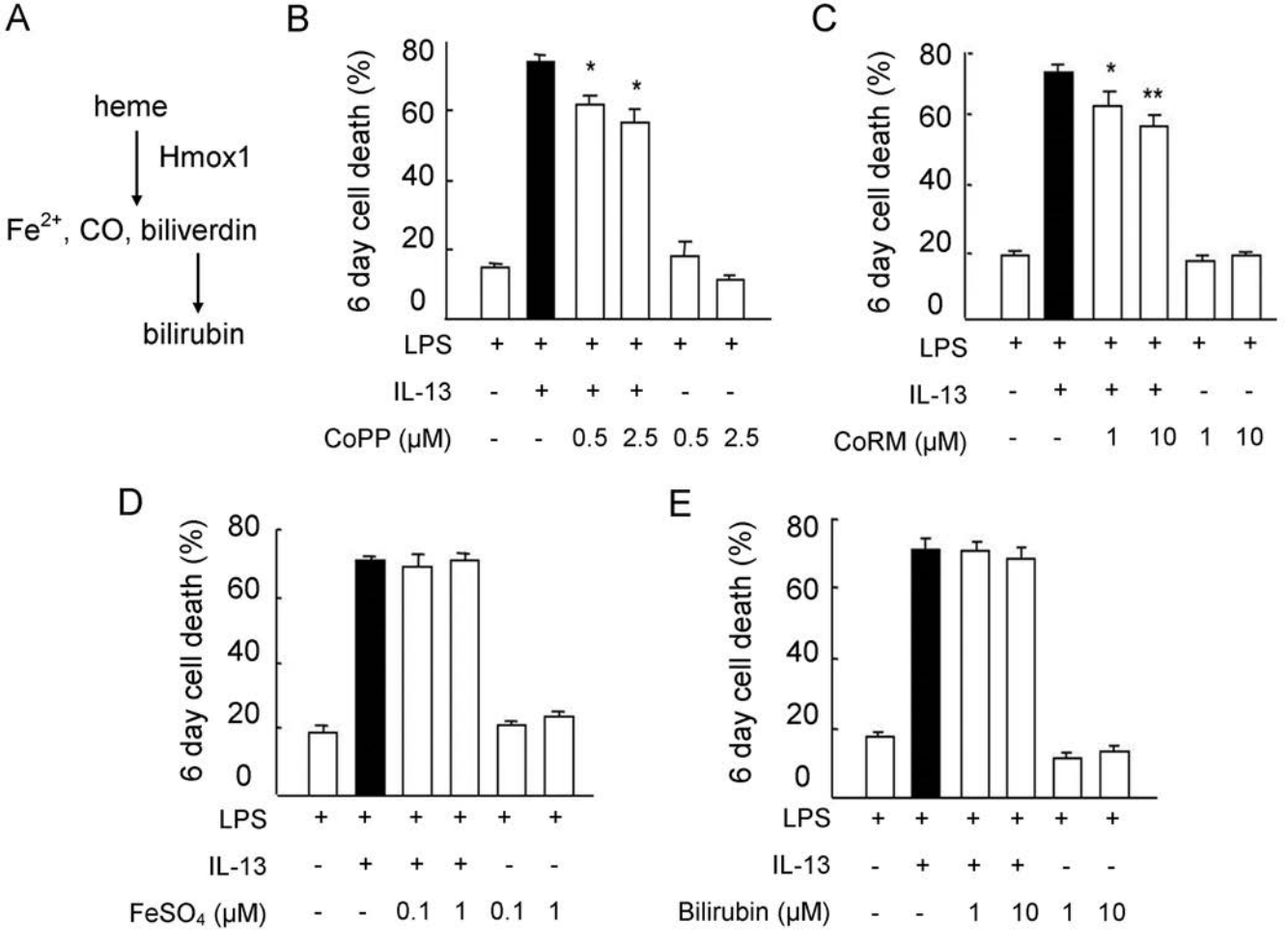
A
heme
Hmox1
Fe2+, CO, biliverdin
bilirubin
B
6 day cell death (%)
80
60
40
20
0
*
*
LPS + + + + + +
IL-13 - + + + - -
CoPP (μM) - - 0.5 2.5 0.5 2.5
C
6 day cell death (%)
80
60
40
20
0
*
**
LPS + + + + + +
IL-13 - + + + - -
CoRM (μM) - - 1 10 1 10
D
6 day cell death (%)
80
60
40
20
0
LPS + + + + + +
IL-13 - + + + - -
FeSO4 (μM) - - 0.1 1 0.1 1
E
6 day cell death (%)
80
60
40
20
0
LPS + + + + + +
IL-13 - + + + - -
Bilirubin (μM) - - 1 10 1 10

Figure 4

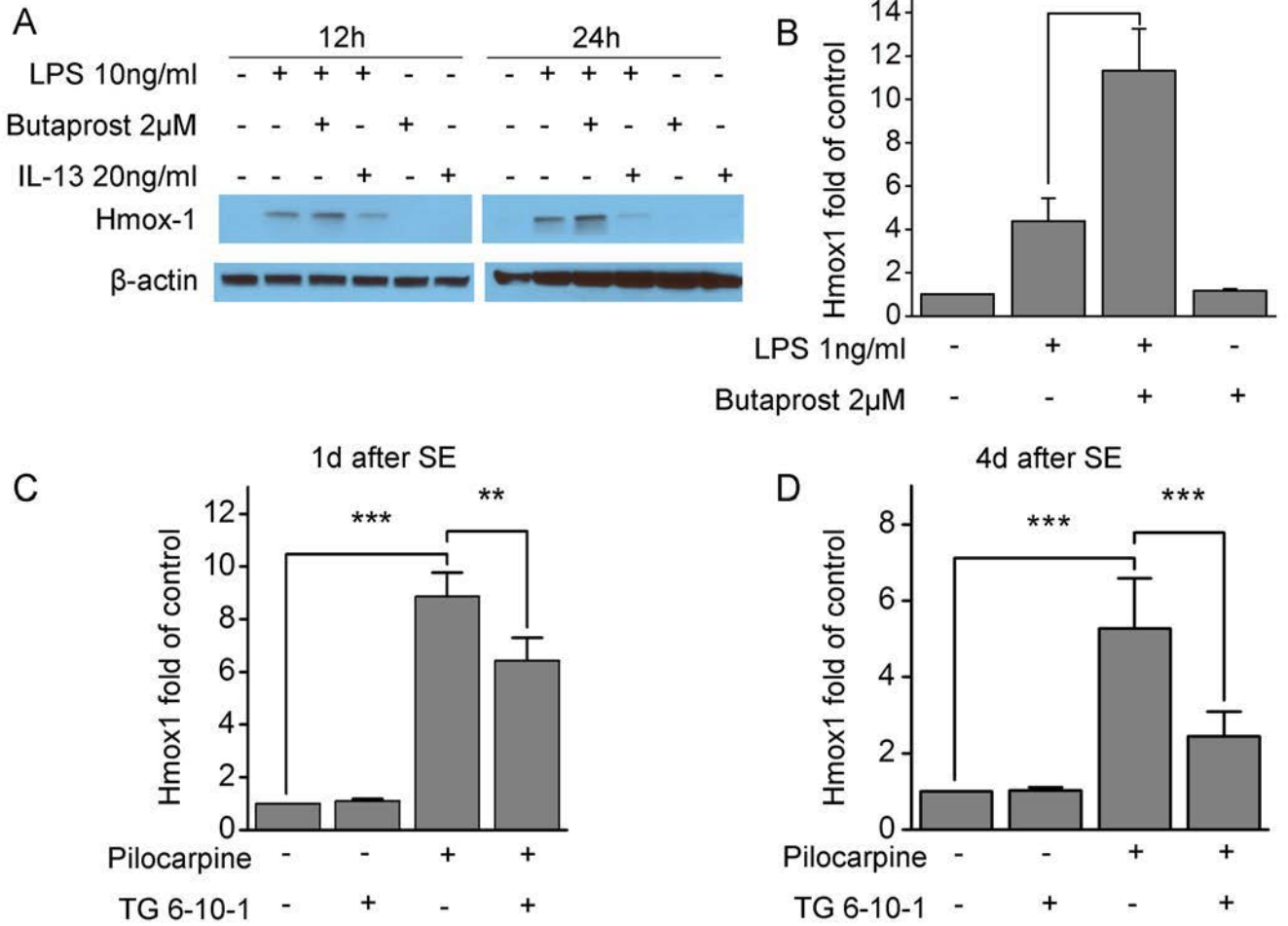
A
12h
24h
LPS 10ng/ml
Butaprost 2μM
IL-13 20ng/ml
Hmox-1
β-actin
B
***
Hmox1 fold of control
LPS 1ng/ml
Butaprost 2μM
C
1d after SE
***
**
Hmox1 fold of control
Pilocarpine
TG 6-10-1
D
4d after SE
***
***
Hmox1 fold of control
Pilocarpine
TG 6-10-1

Figure 5

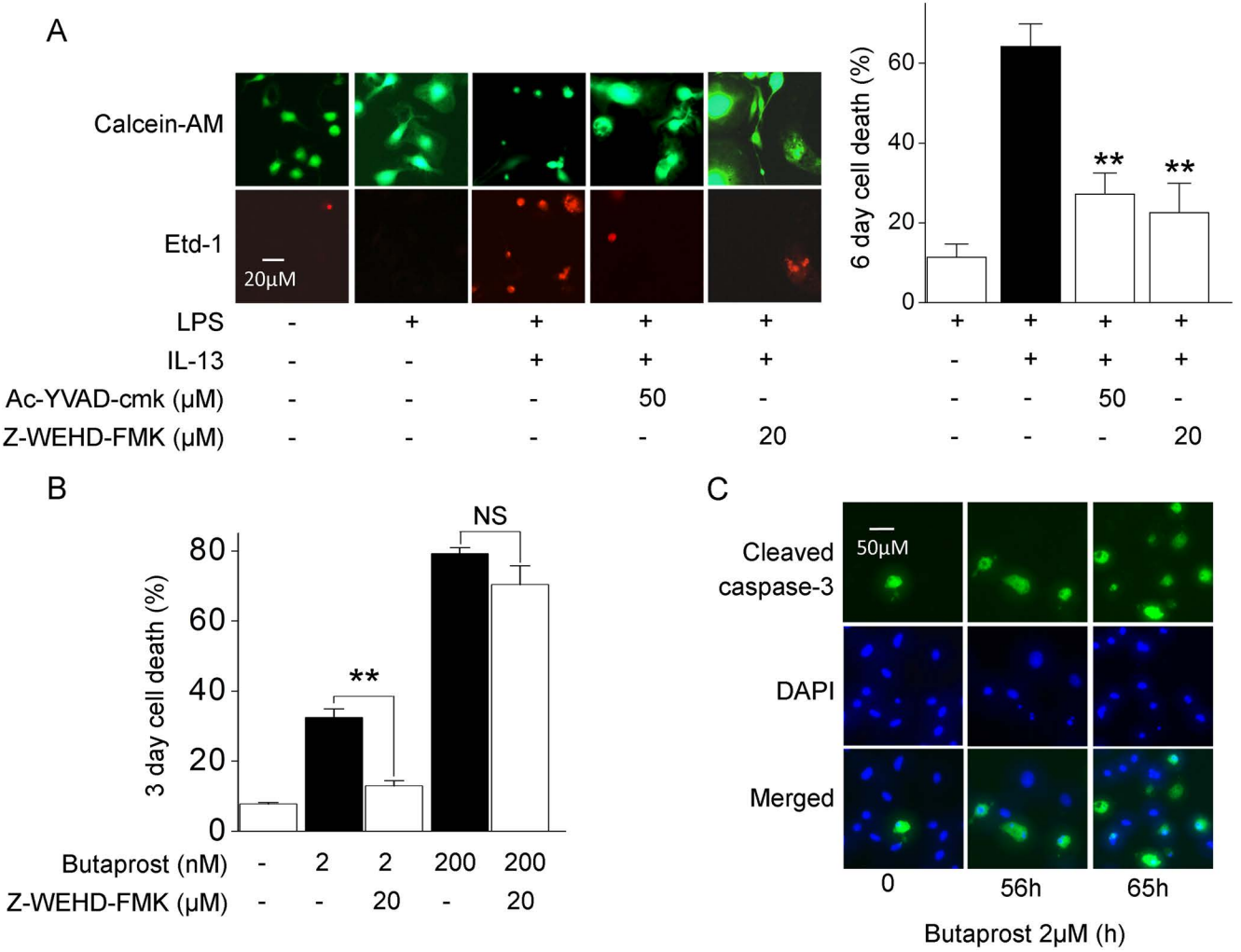
A
Calcein-AM
Etd-1
20μM
LPS - + + + +
IL-13 - - + + +
Ac-YVAD-cmk (μM) - - - 50 -
Z-WEHD-FMK (μM) - - - - 20
6 day cell death (%)
0
20
40
60
**
**
+ + + +
- + + +
- - 50 -
- - - 20
B
3 day cell death (%)
0
20
40
60
80
**
NS
Butaprost (nM) - 2 2 200 200
Z-WEHD-FMK (μM) - - 20 - 20
C
Cleaved caspase-3
DAPI
Merged
50μM
0
56h
65h
Butaprost 2μM (h)

Figure 6

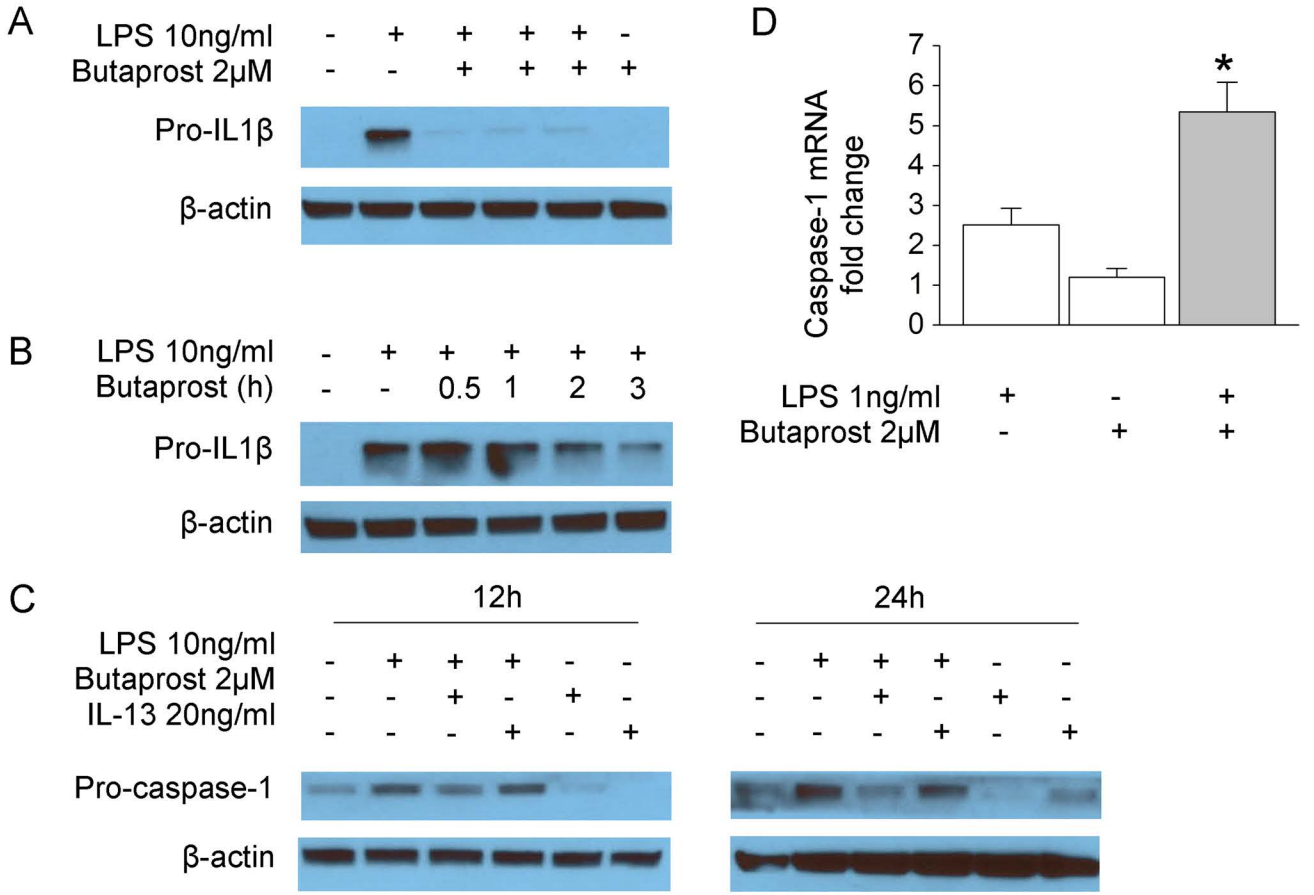
A
LPS 10ng/ml - + + + + -
Butaprost 2μM - - + + + +
Pro-IL1β
β-actin
B
LPS 10ng/ml - + + + + +
Butaprost (h) - - 0.5 1 2 3
Pro-IL1β
β-actin
C
12h
24h
LPS 10ng/ml
Butaprost 2μM
IL-13 20ng/ml
Pro-caspase-1
β-actin
D
Caspase-1 mRNA fold change
0 1 2 3 4 5 6 7
*
LPS 1ng/ml + - +
Butaprost 2μM - + +

Figure 7

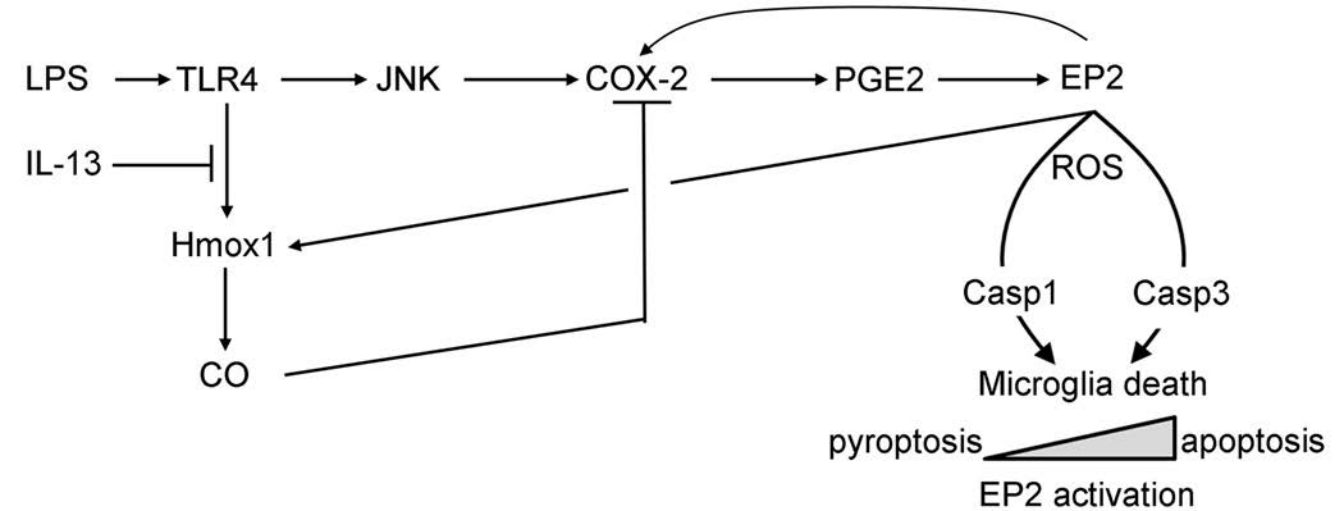
LPS
TLR4
JNK
COX-2
PGE2
EP2
IL-13
ROS
Hmox1
Casp1
Casp3
CO
Microglia death
pyroptosis
apoptosis
EP2 activation

Figure 8